Available online at www.sciencedirect.com
SCIENCE DIRECT®
International Journal of Mass Spectrometry 238 (2004) 17–31
International Journal of Mass Spectrometry
www.elsevier.com/locate/ijms

Review

Chemical properties of mass-selected coinage metal cluster anions: towards obtaining molecular-level understanding of nanocatalysis

Young Dok Kim*

Department of Physics, University of Konstanz, D-78457 Konstanz, Germany

Received 31 May 2004; accepted 3 August 2004
Available online 11 September 2004

Abstract

The catalytic activity of metal clusters often shows an interesting cluster size selectivity, e.g., metals which are inert in bulk form can become extraordinarily catalytically active with reduced cluster sizes. To shed light on elementary steps of catalytic processes on nanoclusters, the chemisorption properties of mass-selected coinage metal cluster anions in the gas phase were studies using time-of-flight (TOF) mass-spectrometry and ultraviolet photoelectron spectroscopy (UPS). In surface chemistry, it is generally accepted that O_2 dissociates at room temperature; however, on coinage metal cluster anions, di-oxygen species can be found, implying that di-oxygen species on coinage metal clusters are important reaction intermediates for the catalytic CO-oxidation and partial oxidation of hydrocarbons. For H adsorption on Au cluster anions, H acts as a one-electron donor like Au does. The implication of this result on heterogeneous catalysis of nanoclusters is discussed.

Keywords: Metal cluster; Oxygen; Chemisorption; Photoelectron spectroscopy

Contents

* Tel.: +49 753188 4682; fax: +49 753188 3888.
E-mail address: young.kim@uni-konstanz.de.

1387-3806/$ – see front matter © 2004 Elsevier B.V. All rights reserved.
doi:10.1016/j.ijms.2004.08.001

1. Introduction

The chemical properties of a cluster can drastically change with increasing number of atoms in a cluster. The rates of the chemisorption of H_2, D_2, and N_2 on Fe_n, and Nb_n (n = number of atoms) clusters and those of CO on different metal clusters can vary by several orders of magnitudes as a function of n [1–6]. For W_n, a sharp jump of the reactivity towards N_2 chemisorption is detected at liquid nitrogen temperature as well as room temperature as n exceeds 15 [7,8]. The reaction pattern of V cluster cations with O_2 drastically changes with increasing number of V atoms in a cluster [9]. Pt cluster cations also show size dependent changes of the activities towards reactions with various gas molecules, such as NH_3, H_2 and O_2 [10,11]. Recently, variations of the chemical properties of mass-selected metal clusters have attracted particular attention of chemists and physicists, since studies on mass-selected clusters were shown to be able to provide a better understanding of elementary steps of heterogeneously catalyzed reactions on nanoparticles, which is currently one of the most important subjects in surface chemistry and heterogeneous catalysis. Using gas-phase clusters, the variations of catalytic activities with increasing cluster size can be studied on an atom-by-atom basis. Moreover, the results from the mass-selected clusters can be directly compared with theoretical calculations, which is difficult for the model catalysts consisting of metal nanoparticles with certain size distributions supported by oxide surfaces. At the beginning of this article, a brief summary will be given, outlining recent efforts of surface chemists to discover unique catalytic properties of nanoparticles, which cannot be found for the bulk counterparts. Furthermore, still open questions from surface chemistry on nanocatalysis will be reviewed. In order to shed light on the questions from a surface chemistry point of view, the chemical properties of mass-selected clusters in the gas phase have been investigated in cooperation with Prof. Ganteför's group of the University of Konstanz, Germany. The results will be reviewed in the present article.

2. Surface science studies on nanocatalysis

One of the most important goals in surface chemistry is obtaining a better understanding of mechanisms of various heterogeneously catalyzed reactions. To unveil the reaction mechanisms on the atomic scale, surface scientists have been using metal single crystal surfaces as model catalysts.

In contrast to the real catalysts consisting of metal nanoparticles on high surface area support materials, such as silica, alumina, magnesia and titania, the experimental parameters in the model catalysts are well-defined, and can be controlled more precisely. Therefore, elementary steps of catalytic processes in these ideal model systems can be investigated on the atomic scale by using various surface analysis techniques under ultrahigh vacuum (UHV) conditions [12–15].

There have been concerns whether the model studies of catalysis can properly describe the real catalysis, and much effort has been made to mimic the complexity of real catalysis in the model studies in order to bridge the gaps between the model and real catalysis. Experimental techniques have been developed, which allow investigations on catalytic processes not only under UHV conditions, but also under high pressure conditions to overcome the "pressure gap" [16–18]. Instead of studying catalytic activities of metal single crystal surfaces, metal particles deposited on oxide single crystalline surfaces have been studied to bridge the "material gap" [19,20]. Oxides are often insulating, thus causing charging problems in many surface analysis techniques, such as electron spectroscopy and scanning tunneling microscopy (STM). This can be avoided by using oxide thin films on refractory metal single crystal surfaces [19,20].

Studies on metal nanoparticles over oxide surfaces revealed that there are actually some examples of nanosized metal particles showing completely different catalytic properties from the bulk counterparts. One of the most well-known examples for this "material gap" is Au-based catalyst. Au is known to be the most inert metal in bulk form; however, Au nanoparticles as large as 2–3 nanometers (nm) have been shown to be extraordinarily active for various catalytic reactions, such as low-temperature CO-oxidation and partial oxidation of hydrocarbons [21–32]. Recently, Ag nanoparticles with an average size of 2–3 nm were also shown to be catalytically as active as the Au nanoparticles [33]. It is likely that the size dependent change of the catalytic activity is not limited to Au, but may be also valid for other materials. It should be noted that there are two most important factors for the efficiency of the nanocatalysts, namely cluster size and metal support interactions: as mentioned above, the catalytic activity can change drastically with cluster size. Metal nanoparticles with the same size show dissimilar catalytic activities, depending on the support material, e.g., catalytic reactions of Au nanoparticles on titania take place at lower temperatures compared to those on silica [22].

Most of the Au-based catalysts used in surface science studies have certain particle size distributions, which do not allow investigations of cluster size selectivity in catalytic reactions on an atomic-by-atom basis. Hence, mono-disperse surfaces are required, i.e., all the clusters deposited on a support material should have the same size. This has been realized by Heiz and co-workers, who deposited mass-selected clusters on oxide thin films [34–36]. Using this technique, Heiz and co-workers found that Au clusters consisting of 8–20 atoms are reactive towards CO-oxidation, when they are deposited on MgO(1 0 0) surfaces [34]. In combination with density functional theory (DFT)-calculations, it was suggested that the Au clusters on stoichiometric MgO surfaces are almost inert, whereas the Au clusters interacting with defect sites of MgO (oxygen vacancies, so-called F-centers) are catalytically active, indicating that strong metal-support interactions play a pivotal role for catalytic activities of nanoclusters [34].

These results from surface science studies triggered further investigations on the chemical properties of mass-selected clusters in the gas phase [37–43]. One of the advantages of studying gas phase clusters is that they can be more easily mass-separated than deposited clusters. Note that for deposited clusters, diffusion of the clusters on the substrate surfaces can take place, which may lead aggregations of the clusters (sintering). To avoid this problem, suitable experimental parameters, such as low deposition temperatures and low cluster coverages should be chosen. It is also important to mention that by comparing chemical reactivities of gas phase clusters to those of the respective deposited clusters, one can better understand metal-support interactions. Many cluster chemists and physicists have been investigating the chemical properties of mass-selected cluster in the gas phase, e.g., Whetten and co-workers found that Au cluster anions in the gas phase are as active towards CO-oxidation as deposited Au nanoclusters, suggesting that gas phase clusters can be used as model systems to gain insights into the elementary steps of various catalytic reactions [37,42].

Catalytic reactions involve many elementary steps. It is a generally accepted view that adsorption and activation of O_2 is the most important step in various catalytic reactions, particularly in low-temperature CO-oxidation. When atomic oxygen instead of molecular oxygen is deposited on Au-based catalysts, CO can readily react with the atomic oxygen to form CO_2, independently on the cluster size, i.e., the size dependent changes of the chemical activities completely disappear in this case [44]. This result of the Bullins' group obviously shows that chemisorption and activation of O_2 on Au-based catalysts are the keys of the cluster size selectivity of Au-nanocatalysis [44]. The nature of the chemisorbed oxygen has been in debate. Dissociative and molecular chemisorption of O_2 were suggested from various previous studies; however, direct experimental evidence on this issue has been missing [34,37,44–51]. Only very recently, spectroscopic measurements on the reacted cluster anions allowed identification of the structures of the oxygen attached to the coinage metal cluster anions [52–56]. Most of this article is devoted to the O_2 chemisorption on coinage metal cluster anions. The last part deals with the hydrogen adsorption on Au cluster anions, which can be relevant for the catalytic reactions involving hydrogen chemisorption, such as partial oxidation of propylene to propylene oxide [57].

3. Experimental set-up

To synthesize $M_nO_2^-$ (M = metal atom), a pulsed arc cluster ion source (PACIS) was used [58,59]. In the PACIS source, a He pulse is inserted between the target and Mo (or W) electrodes, and a high voltage (about 100 V) between two electrodes ignites an electric arc, leading to the sputter-process of the target electrode. The metal atoms ejected from the target electrode can be thermalized to room temperature during collisions with a carrier gas (He), and at the same time, these atoms form clusters. After the clusters have cooled down to about room temperature, they are exposed to O_2 to study the oxygen chemisorption properties of the mass-selected clusters. In the case of hydrogen chemisorption on Au cluster anions, H_2 was inserted into the electric arc, resulting in dissociation of H_2. H_2 does not react with Au cluster anions at room temperature; in contrast atomic hydrogen produced in this way can react with Au cluster anions. We have also performed experiments on $M_nO_2^-$ (M: Au, Ag and Cu), which were produced by inserting O_2 into the electric arc, so that atomic oxygen and metal atoms can thermalize simultaneously and form clusters; however, the results from these experiments are out of scope of the present article. By measuring the UPS peak widths of Cu clusters created in the PACIS source, the temperature of the clusters at the stage of UPS measurements was estimated to be room temperature [58]. The mass of cluster anions was selected using a time-of-flight (TOF) mass spectrometer, and the ultraviolet photoelectron spectra (UPS) of the mass-selected cluster anions were taken using UV laser pulses (photon energy = 4.66 or 6.4 eV). The energy resolution of our UPS instrument is about 0.1 eV.

4. Results and discussion

4.1. O_2 chemisorption on Au cluster anions

4.1.1. O_2 chemisorption reactivity of Au cluster anions

In Fig. 1, mass spectra of Au_n^- after reaction with O_2 are given [52,53]. The grids in Fig. 1 correspond to the masses of the pure Au clusters, and peaks deviating from the grids come from the reacted clusters. Au_n^- with n = even numbers react with O_2 (with an exception of Au_{16}^-), whereas the odd numbered clusters are inert (with exceptions of Au_1^- and Au_3^-, which partially react). Our results are in agreement with the even/odd-alternation in the O_2 adsorption reactivities, which were previously observed by Lee and Ervin [43]. The even/odd-alternation of the O_2 chemisorption reactivity

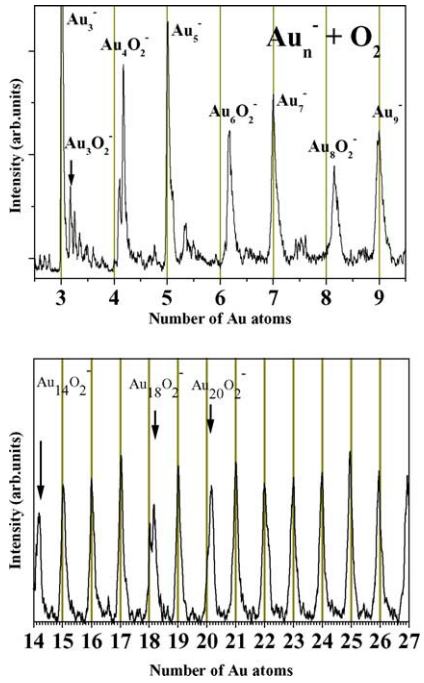

Fig. 1. TOF mass spectra of Au cluster anions reacted with O_2. The grids correspond to the masses of the pure Au clusters, and thus the peaks deviating from the grids come from the reacted clusters.

correlates with the even/odd-pattern of the adiabatic electron affinity of Au_n (in the present work, the electron affinity is defined as the energy difference between the ground state of the anionic cluster and that of the neutral cluster). Note that electron affinities of the even-numbered Au_n are generally lower than those of the directly neighboring odd-numbered clusters [38,60]. It is important to mention that Au_n^- with n >20 do not react with O_2 at all.

The even/odd-alternation of the electron affinities of Au clusters can be understood based on a simple electronic model. Au has one 6 s electron in the valence shell structure, and thus, the highest occupied molecular orbitals (HOMOs) of even-numbered Au cluster anions consist of a hole and an unpaired electron (open shell configurations), whereas those of odd-numbered Au cluster anions are occupied by two paired electrons, i.e., the HOMOs are closed. Note that as mentioned above, the even-numbered Au clusters with open shell configurations have lower electron affinities than the odd-numbered neighbors with closed valence shells [60]. The results of the chemisorption experiments in Fig. 1 indicate that only those cluster anions with lower electron affinities having open valence electronic structures can generally react with O_2 efficiently, whereas the Au clusters with closed shell configurations are less reactive. The results that the Au cluster anions consisting of more than 20 atoms are inert can be also rationalized with the electronic model, since these larger clusters with even as well as odd numbers of Au atoms have relatively high electron affinities compared to those of the smaller even-numbered Au clusters [60]. Chemisorption of O_2 can result in various oxygen-species, such as O_2^- (superoxo-species), O_2^{2-} (peroxo-species) and dissociatively chemisorbed oxygen. The even/odd-alternation in the chemisorption reactivity of O_2 can be interpreted in the following way: O_2 acts as a one-electron-acceptor, thus yielding closed-shell configurations of the even-numbered Au cluster anions upon attachment of an O_2 molecule. Considering that the superoxo-species is a one-electron acceptor, the results in Fig. 1 imply that oxygen is non-dissociatively bound on the Au cluster anions [37,38]. It is interesting to note that the degradation reactions of the Au cluster cations with NH_3 and CH_3NH_2 also exhibit pronounced even–odd behaviours, implying that the chemistry of coinage metal cluster anions is often dominated by their electronic structures [61].

4.1.2. UPS studies on O_2 chemisorption on Au cluster anions (photon energy = 4.66 eV)

In Fig. 2, the UPS spectra of $Au_nO_2^-$ with n = 1, 2, 4, 6, 8 taken using a laser with a photon energy of 4.66 eV are compared [52,53]. UPS spectra for $Au_nO_2^-$ with n = 2, 4, 6 exhibit vibrational fine structures of about 150–180 meV corresponding to the O–O stretching frequencies, indicative of non-dissociative adsorption of O_2. For n = 8, the vibrational fine structure is not discriminated. The vibrational frequencies in Fig. 2 are much higher than those of the dioxygen species on transition metal surfaces. Note that the vibrational frequencies of molecular oxygen species on transition metal surfaces are 80–120 meV for peroxo-species and 135–150 meV for superoxo-species [62,63]. The vibrational frequency in the UPS spectra of a cluster anion corresponds to that of the neutral cluster having the ground state geometry of its respective anion. As nuclear motions are generally much slower compared to the detachments of electrons, the so-called vertical detachment takes place, which results in neutral clusters with the same geometries as that of the anion ground states as final states of the photoelectron emission processes. In the anionic states, the additional electrons occupy the antibonding $2\pi^*$ orbitals of O_2, thus further activating the O–O bonds, and decreasing the O–O stretching frequencies.

Since we observe strong vibrational structures of O–O, the O–O bond length should be significantly altered upon the one electron detachment. The additional electron in the anionic state is strongly localized on oxygen, in line with recent theoretical studies, which found strong resonances of the O_2-$2\pi^*$ and HOMOs of the Au cluster anions [64].

UPS spectra do not provide information on geometric structures of the clusters, yet comparison with density functional theory-calculations can shed some light on the cluster geometry. In Fig. 3, the optimized geometries of $Au_nO_2^-$ with n = 2, 4 by theoretical calculations of Jena's group are given [54]. For the theoretical studies, the self-consistent linear combination of atomic orbital–molecular orbital (SCF-LCAO-MO) approach was used. The total energies are calculated using DFT with the generalized gradient approximation (GGA) for the exchange-correlation potential, which is

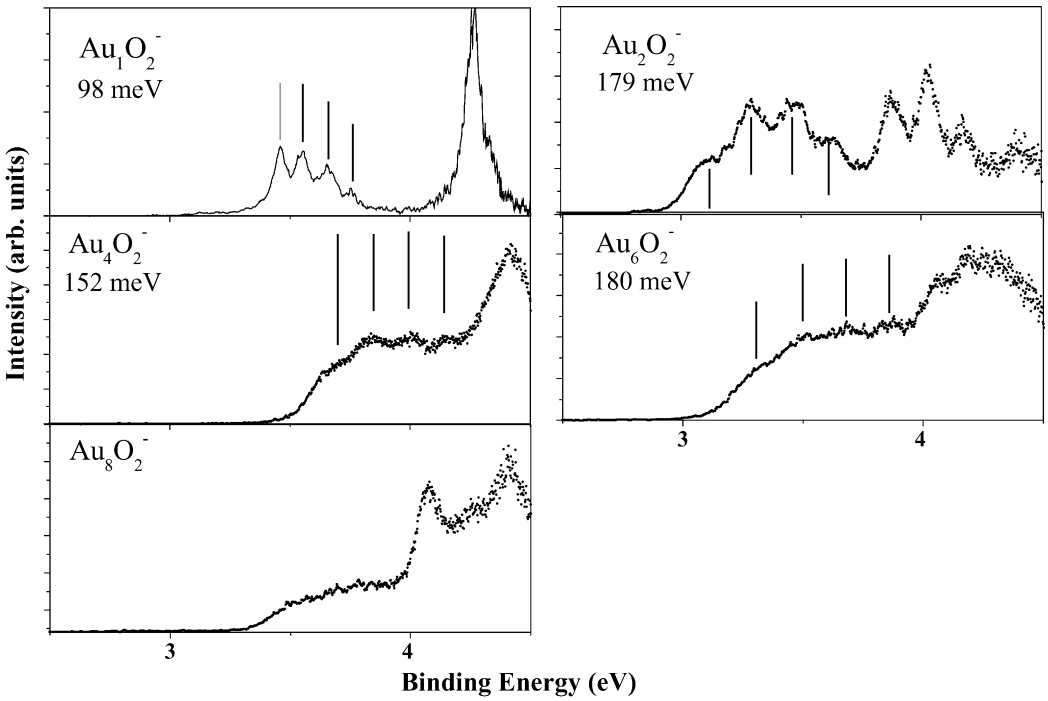

Fig. 2. UPS spectra of $Au_nO_2^-$ with n = 1, 2, 4, 6, 8. The photon energy is 4.66 eV. Vibrational fine structures are denoted in the figure.

taken as Perdew-Wang 91 prescription (commonly referred to as PW91). The atomic orbitals are represented by a Gaussian basis. The 6-311++G (3df, 3pd) basis set for O and the Stuttgart relativistic effective core potential basis set for Au were used. The structures for the anionic and neutral clusters were optimized without symmetry constraint using the Gaussian 98 code. For both clusters, the formation of superoxo-species was suggested from theory, in line with the experimental data. The theoretically calculated electron affinities of these clusters are in good agreement with the experimental data, suggesting that the theoretical approach used here is highly reliable [54]. The O–O distances in these clusters are about 1.3 Å, which is larger than those of the neutral counterparts by about 0.05 Å. This result also reveals that the excess electrons in the negatively charged Au clusters play an important role for the activation of the O–O bonds.

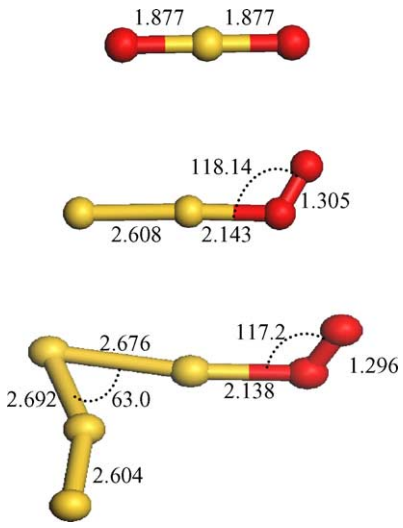

Fig. 3. Optimized geometric structures of $Au_nO_2^-$ with n = 1, 2, 4 using DFT-calculations. Bond lengths and angles (in degree) are given in the figure.

For the Au monomer anions, the vibrational frequency is much lower than those of the other clusters in Fig. 2. It is difficult to provide a clear interpretation of this result, since 98 meV can be assigned either to the Au–O or the O–O stretching frequency. In this case, therefore, combined studies with DFT-calculations are required. In the DFT-calculations for the Au monomer anions, dissociative adsorption of oxygen on Au, forming a linear O–Au–O^- structure is energetically more favorable than the molecular adsorption by about 0.7 eV, suggesting dissociative chemisorption of oxygen. Again, the electron affinity, the vertical detachment energy (VDE) and the vibrational frequency of AuO_2^- from the theoretical calculations are consistent with the experimental data [54]. It is, however, remarkable that according to the theoretical calculations of Jena's group, the dissociation of O_2 on Au, is impeded by a large activation barrier, which cannot be overcome at room temperature [54]. Therefore, it is likely that the formation of AuO_2^- results from reactions between Au^- and small amounts of atomic oxygen (or hot molecular oxygen) being present in the gas phase.

4.1.3. UPS studies on O_2 chemisorption on Au cluster anions (photon energy = 6.4 eV)

UPS studies using a laser with a photon energy of 4.66 eV are limited to the smaller reacted clusters consisting of less

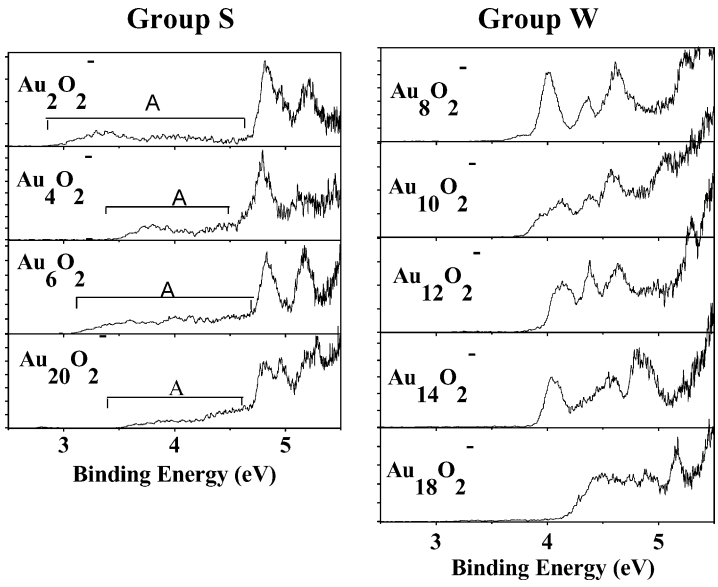

Fig. 4. UPS spectra of $Au_nO_2^-$ with n = 2, 4, 6, 20 (the group S) and n = 8, 10, 12, 14, 18 (the group W). The photon energy is 6.4 eV.

than 10 Au atoms, since the electron affinities of the larger clusters become very close to the photon energy. To obtain information on electronic structures of $Au_nO_2^-$ for $n < 21$ with a wider energy range, UPS spectra of $Au_nO_2^-$ are collected using a laser with a higher photon energy (6.4 eV) (Fig. 4) [53,54]. Based on the shapes of the UPS spectra, $Au_nO_2^-$ clusters studied here are classified to two different groups (S and W groups), where S stands for stronger Au–O interactions, and W for weaker Au–O interactions.

First, we focus on $Au_nO_2^-$ clusters with n = 2, 4, 6, 20 (referred to as group S). The respective bare Au clusters of this group show relatively low electron affinities (<2.75 eV) [60]. The distinct features of the pure Au cluster anions existing at the binding energies below about 4.7 eV completely disappear upon O_2 adsorption, and broad features between 3 and 4.5 eV (marked with A in Fig. 4) can be found, followed by several narrower peaks at higher binding energies. These broad features denoted as A in Fig. 4 result from the combination of the O_2-2π*-orbitals and the valence occupied MOs of Au_n^-. As mentioned above, O_2 molecularly adsorbs on Au_n^- with n = 2, 4, 6 (Fig. 2), and based on the similarities in the valence electronic structures (Fig. 4), O_2 is suggested to be also molecularly bound on Au_{20}^-, forming superoxo-species. The very large widths of the peaks A are evidence for a strong overlap of the O_2-2π* orbitals with the valence electronic levels of Au_n. Note that according to the Franck–Condon profile, a large structural change upon electron excitation results in broad band features: an electron detachment can lead to a large structural change, when this electron is involved in a strong chemical bonding of a cluster (in our case O_2–Au bonding), which can lead to the appearance of broad features in the photoelectron spectra. By comparing the UPS spectra of the $Au_nO_2^-$ with those of the respective pure Au cluster anions (Fig. 5), it becomes more obvious that the valence band structure of Au_n^- is completely changed upon O_2 adsorption, confirming significantly large interactions between O_2 and Au in the group S clusters. It should be noted that not only HOMO but also other occupied MOs of the Au cluster anions participate in the O_2 chemisorption (Figs. 4 and 5). Most likely, the approach of O_2 close to Au_n^- is facilitated by sufficient charge transfers from the delocalized sp-state (HOMO) to the O_2-2π* orbital, which then enables the contributions of other localized MOs of Au_n^- with higher binding energies in the O_2 chemisorption.

In contrast to the case of the group S clusters, the UPS spectra of $Au_nO_2^-$ with n = 8–18 (group W) consist of distinct multiple peaks (Fig. 4). The peaks from the HOMO of the bare Au cluster anions disappear upon O_2 adsorption; however, in contrast to the case of the group S, no broad feature is observed in the binding energy regime between 3 and 4.5 eV. Only distinct peaks above 4 eV existing in the UPS spectra of the pure Au cluster anions are still visible with minor modifications after O_2 adsorption (Fig. 5). This suggests that charge transfers from the HOMO of the Au cluster anions to oxygen is the main chemisorption mechanism, whereas an additional overlap between the O_2-2π* orbital and other MOs of the Au cluster anions is negligibly small, which is quite different from the results of the group S clusters (Figs. 4 and 5). This result is evidence for much weaker interactions between O_2 and Au in the group W clusters compared to those of the group S clusters. The general trend for the weaker interactions of the group W clusters with O_2 is consistent with the recent results from the O_2 adsorption reactivity experiments on Au cluster anions described in [38]. Much weaker interactions between O_2 and Au in the group W clusters imply non-dissociative chemisorption of O_2 in the group W, since for the dissociative adsorption, stronger Au–O_2 interactions are required. That the Au cluster anions in the group W react more weakly with O_2 than in the case of the group S is

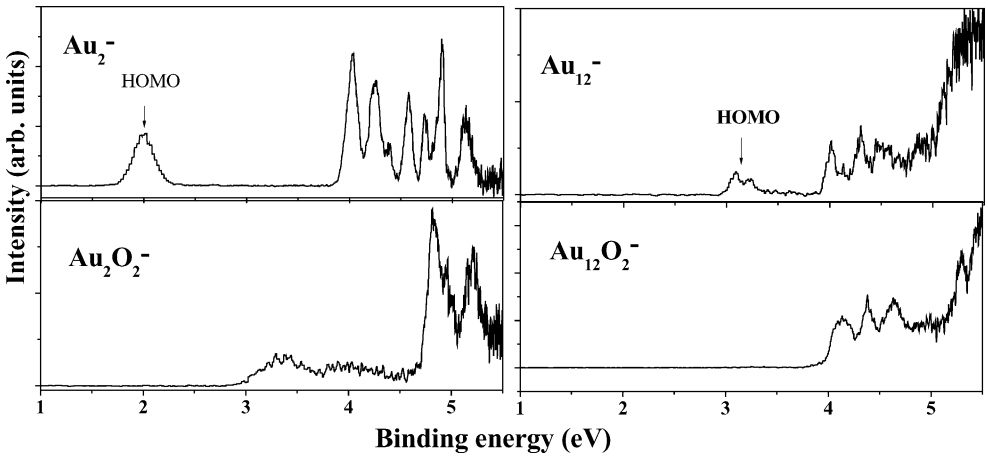

Fig. 5. The UPS spectra of Au_n^- and $Au_nO_2^-$ (n = 2, 12) are compared. The photon energy is 6.4 eV.

explained by the lower electron affinities of the bare Au clusters of the group S compared to those of the group W [60], because within a simple charge transfer model, one can argue that the W group clusters allow less Au → O_2 charge transfer than the S group clusters.

It is interesting to note that the O_2 adsorption mechanism on Au_{20}^- is much different from that of other Au cluster anions with similar sizes (Au_n^- with $n > 8$), and rather analogous to the O_2 adsorption pattern of much smaller clusters (n = 2, 4, 6). Au_{20} has a highly symmetric tetrahedral structure with a HOMO-LUMO gap of 1.8 eV, which is the largest among coinage metal clusters studied so far, except Au_6, i.e., Au_{20} is classified as a "magic" cluster, suggesting that Au_{20} should be chemically inert [65]. In general, "magic" clusters tend to exhibit relatively low electron affinities, since the energy level of LUMO is shifted to the lower binding energy range as a consequence of a large HOMO-LUMO gap [66]. The strong interaction with Au_{20}^- with O_2 indicates that a "magic" cluster can become chemically very active with an excess electron, triggering further studies on chemical activities of other "magic" clusters with one excess electron. It should be emphasized that it is not only the one additional electron in the HOMO of the anionic state of the "magic" cluster, which participates in the chemisorption. Other MOs in the higher binding energies, which should be chemically inert in the neutral state, participate in the chemisorption in the anionic state.

4.1.4. Reaction mechanisms

Under similar experimental conditions to those of ours (room temperature, comparable O_2 partial pressure), Au_2^-, Au_4^- and Au_6^- clusters were shown to be highly reactive towards oxidation of CO to CO_2 [37,42]. Comparison of the chemisorption properties of Au_n^- with those of the Pt-group metal surfaces provides insights into the origin of the unusual catalytic properties of Au nanoclusters for CO-oxidation and propylene epoxidation. Pt-group metals can efficiently catalyze CO-oxidation, but the operating temperatures of Pt-group catalysts are known to be significantly higher than those of the Au-nanocatalysts. On Pt-group metal surfaces, CO-oxidation usually takes place through the dissociative chemisorption of O_2 to atomic oxygen, which subsequently reacts with CO to form CO_2 [67]. On the Au cluster anions, in contrast, the stabilization of the activated molecular oxygen at room temperature can open up new reaction channels (e.g., CO-oxidation mediated by carbonate-like species), responsible for the low temperature CO-oxidation [37,38,42,46]. Molecular adsorption of oxygen can play a vital role for the enhanced activities of Au clusters towards many other catalytic reactions, such as partial oxidation of propylene, in which formation of hydrogen peroxide (HOOH) is suggested to be important [31]. It should be mentioned that non-dissociative chemisorption seems to be a general phenomenon for small nanoclusters, and therefore many other catalytic reactions may proceed via non-dissociatively chemisorbed species on nanoclusters. For example, N_2 chemisorbs dissociatively on W surfaces [13], but molecularly on W nanoclusters consisting of less than 15 atoms [68,69]. Stabilization of di-nitrogen and di-hydrogen species on small nanoclusters was also found on Nb and Ti cluster anions, respectively [70]. For ammonia (NH_3) synthesis on metal surfaces, it is generally accepted that N2 dissociatively chemisorbs and then reacts with H, however, on small nanocatalysts, it is possible that di-nitrogen species are formed [13,71]. Di-nitrogen species can react with H to form N–N–H_n (n = 1–3), which upon further hydrogenation can then decompose to form NH_3 [71].

It is unclear so far, if the CO-oxidation on the Au cluster anions operate via the Langmuir–Hinshelwood mechanism, or the Eley–Rideal mechanism. In the Langmuir–Hinshelwood mechanism, CO and O_2 both chemisorb on catalyst surfaces, and CO molecules diffuse on the surfaces until they can find thermally activated oxygen atoms to react to CO_2 [67]. In the Eley–Rideal mechanism, CO molecules existing in the gas phase react with surface oxygen species, without forming chemical bond with surface

atoms, i.e., in the Eley–Rideal mechanism, the residence time of CO on the catalyst surface during reactions can be regarded to be 0 s [72]. In surface chemistry, it has been suggested that CO-oxidation can take place via the Eley–Rideal mechanism on oxygen-rich Ru surfaces [73,74]; however, this suggestion later turned out to be invalid [75]. No direct evidence has been observed for the CO-oxidation on metal surfaces taking place via the Eley–Rideal mechanism, which thereafter has been rather regarded as an unrealistic mechanism for heterogeneous catalysis [15]. In this context, it is worth mentioning that CO-oxidation on Au clusters is suggested to occur by the Eley–Rideal mechanism in recent theoretical calculations, and it could be interesting to find experimental evidence on this issue [42].

4.1.5. Metal-support interactions

Studies from Whetten and Wallace reported in [37] as well as those in the present work show that metal clusters consisting of less than 20 atoms are reactive towards CO-oxidation. However, according to the finding from Goodman's group, Au particles consisting of about 100–200 atoms are reactive, when they are supported by TiO_2 surfaces [21]. Comparison of the gas phase data and those of the Au particles on TiO_2 can provide a better insight into the role of the support materials in the Au-nanocatalysis. We suggest that support materials in Au-nanocatalyis may play the following roles:

(1) The experimental findings using mass-selected clusters suggest that not only cluster size but also the charge state in a cluster can have significant influence on its chemical properties. From the results shown in the present article, it is evident that negatively charged even-numbered Au clusters are reactive towards O_2 chemisorption. In contrast, cationic Au clusters are inert towards O_2 chemisorption [76]. It is possible that in the case of supported nanoparticles, their charge states can be modified by support materials, as it was suggested by theoretical studies on Au nanoclusters over MgO surfaces [34]. Depending on the support material, Au nanoparticles can have positive, neutral or negative charge, which can significantly alter their chemical activities. It is interesting to note that the X-ray photoelectron spectroscopy (XPS) results from Au particles on TiO_2 in combination with DFT calculations are also suggestive of a negative charging of the chemically active Au particle by a charge transfer from oxygen vacancies of TiO_2 to Au [77].

(2) In the gas phase, the HOMO-LUMO gaps of the clusters become negligibly small (<∼0.2 eV), when the clusters consist of more than about 25–30 atoms [60]. The 2D–3D transition of the Au clusters takes place when the number of Au atoms in a cluster becomes 11–13 [78]. The cluster shape becomes completely three-dimensional at a cluster size of Au_{20} [65]. In contrast, Au strongly wets the TiO_2 surfaces, keeping the confined thickness of larger clusters to the direction normal to the oxide surface (Au initially grows two-dimensional), which increases the contact area between Au and TiO_2 [21]. As a consequence of the metal-support interaction, Au particles consisting of several hundreds Au atoms (about 2–3 nm in diameter) are still semiconductive with band gaps up to 1.2 eV [21]. As aforementioned, a larger band gap (or HOMO-LUMO gap) of a nanoparticle corresponds to a lower electron affinity [66], leading to a higher chemical activity towards O_2 adsorption. This can rationalize, why the mean size of the catalytically active Au particles on TiO_2 is much larger than that in the gas phase without support.

4.2. O_2 chemisorption on Ag cluster anions

4.2.1. Reactivity measurements

In Fig. 6, mass spectra collected for Ag cluster anions after reaction in O_2 environments are displayed [55]. The even/odd-behaviours of Au cluster anions can also be observed for Ag cluster anions, even though there are some exceptions for this even/odd-relationship. For example, in Fig. 6, it is evident that Ag_{16}^- and Ag_{18}^- are less active than other even-numbered Ag cluster anions. It is interesting to note that the even/odd-alternation in the O_2 adsorption reactivities can still be observed for the Ag clusters consisting of more than 30 atoms in Fig. 6 (except Ag_{32}^-), which is

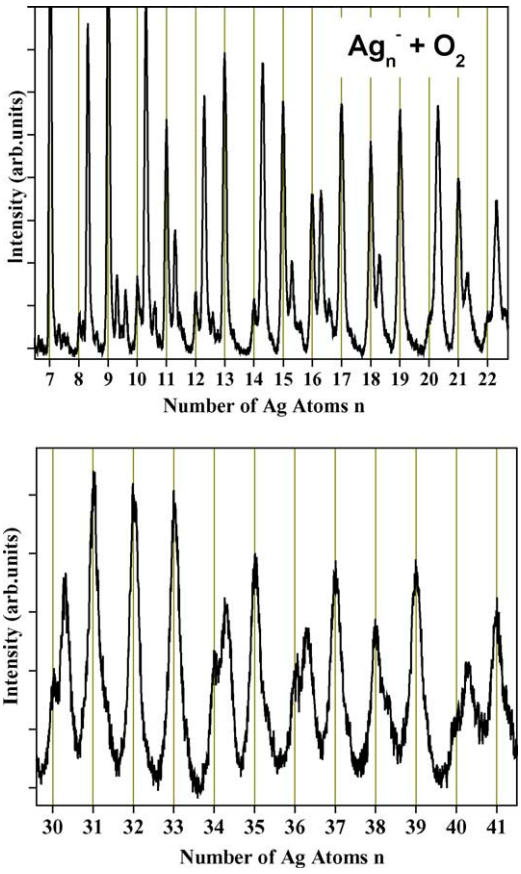

Fig. 6. TOF mass spectra of Ag cluster anions reacted with O_2. The grids correspond to the masses of the pure Ag clusters, and thus the peaks deviating from the grids originate from the reacted clusters.

quite different from the result of Au. Note that the Au cluster anions larger than Au_{20}^- are inert towards O_2 adsorption in Fig. 1.

Analogous to the results of the O_2 chemisorption of Au cluster anions, the even/odd-alternation of the O_2 adsorption on Ag cluster anions can be explained within an electronic model, since the even-numbered Ag cluster anions generally show lower electron affinities with respect to those of the odd-numbered neighbors. The reason for the even–odd alternation in electron affinities as a function of cluster size is mentioned above (Section 4.1.1). The Ag cluster anions with lower electron affinities can facilitate the electron transfer to the antibonding MO of O_2, resulting in higher reactivities towards O_2 adsorption. In contrast, the anionic clusters with higher electron affinities prohibit a charge transfer to the adsorbates under our experimental conditions, hence decreasing the O_2 adsorption activities. As described above, the even/odd-alternation of the O_2 chemisorption reactivity has been regarded as indication of the formation of superoxo-species on Au cluster anions, which was also verified by our UPS experiments. Therefore, the even/odd-behaviours of O_2 chemisorption on Ag cluster anions can also imply that O_2 acts as a one-electron acceptor forming superoxo-species, i.e., O_2 adsorbs non-dissociatively on the Ag cluster anions.

The O_2 chemisorption data of Au cluster anions nearly perfectly correlate with the electron affinity changes (Fig. 1) [38]. Based on the simple electronic model mentioned above, it seems to be reasonable that the Ag cluster anions show an even/odd-behaviour for the O_2 adsorption, analogous to the case of Au, since the valence electronic configurations of the Au and Ag clusters are similar. Note that Au and Ag both have one s electron in the valence atomic orbitals. Our observation that Ag_{16}^- and Ag_{18}^- are less reactive than other even-numbered neighbors also reconciles the relatively high electron affinities of these clusters compared to those of other even-numbered Ag clusters [60]. However, it is important to note that the absolute electron affinities of Ag cluster anions are generally significantly lower that those of the Au cluster anions with similar sizes [60]. The electron affinities of the even-numbered Au clusters consisting of less than 20 atoms, which are active towards O_2 adsorption in the anionic form, are lower than 3.4 eV, whereas the Au clusters inactive in the anionic state have electron affinities above 3.4 eV [60]. The electron affinities of Ag_n with n = even and odd numbers are always <3.2 eV [60]. Assuming that the absolute electron affinity is the only criterion for the reactivity towards O_2 adsorption, not only even-numbered but also odd-numbered Ag cluster anions should be reactive towards O_2 adsorption. However, our experimental observation of the even/odd-behaviours of the Ag cluster anions towards O_2 adsorption suggests that the absolute electron affinity cannot be a sufficient criterion to determine the reactivity towards O_2 adsorption.

Despite the much higher electron affinities of the Au clusters compared to the respective Ag clusters, Au and Ag cluster anions consisting of less than 21 atoms show similar activity patterns towards the O_2 adsorption. Strong d characters in the valence band of the Au clusters may be taken into account to rationalize these results. Previous quantum chemical calculations have found very strong d-sp mixing for Au, and the UPS spectra of the pure Au cluster anions also agree with these calculations [60,79–82]. The stronger d characters of Au nanoclusters are most likely related to relativistic effects [83–85]. As the atomic nuclear charge increases, electrons penetrating to the nucleus increase their velocity, and consequently their mass due to relativity. The relativistic effect causes the s electrons to be in smaller orbitals than one might classically expect. The s electrons are therefore more strongly bound, shielding d electrons more effectively [83–85]. Ample evidence can be found in the literature that the relativistic effect plays a pivotal role in the chemistry of heavy metal atoms like Au [83,85]. Ag valence bands exhibit more sp and less d character compared to those of Au. It is possible that d orbitals play an important role for the chemisorption of O_2, since the d-orbitals can overlap better with O_2-$2\pi^*$ orbitals than the sp-states due to symmetry reasons. Because of the larger d character in the valence electronic levels of Au clusters, even-numbered Au clusters anions can be as reactive as Ag cluster anions for O_2 adsorption, in spite of relatively high electron affinities of even-numbered Au clusters compared to those of the respective Ag clusters.

Larger Ag and Au clusters behave chemically completely different, i.e., Au cluster anions larger than Au_{20}^- are inert towards O_2 adsorption, whereas the Ag cluster anions consisting of more than 20 Ag atoms are still reactive. However, the O_2 adsorption pattern of the Ag cluster anions consisting of less than 21 atoms is quite analogous to the case of the respective Au clusters.

4.2.2. UPS studies

In order to shed light on structural properties of $Ag_nO_2^-$, UPS experiments were carried out (Fig. 7) [55]. Only for $Ag_2O_2^-$ and $Ag_8O_2^-$, periodic structures are observed in the UPS spectra corresponding to about 170 meV, which can be assigned to the stretching frequency of O–O of a superoxo-species (Fig. 7) [68,63]. The observation of the O–O stretching frequency at the lower binding energy regimes in the UPS spectra of $Ag_2O_2^-$ and $Ag_8O_2^-$ indicates that the detachment of the electrons with the lowest binding energies in $Ag_2O_2^-$ and $Ag_8O_2^-$change the O–O distance significantly. This implies that the excess electron in the anionic state should be localized in O_2, which was also found for the O_2 chemisorption on the Au cluster anions by theoretical calculations [64]. For other clusters without vibrational fine structures, direct evidence of chemisorption geometries of O_2 is missing; however, it is important to note that recent theoretical studies on O_2 chemisorption on Ag cluster anions suggest formation of superoxo-species, in line with our interpretation about the even/odd-behaviours of the O_2 chemisorption reactivity experiments [40].

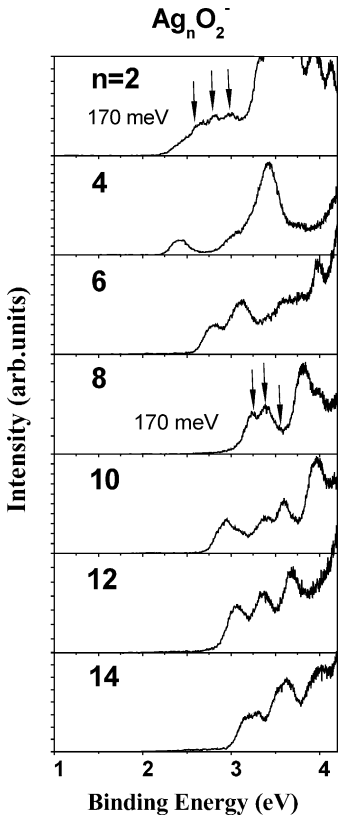

Fig. 7. UPS spectra of the even-numbered $Ag_nO_2^-$ with n = 2–14. The photon energy is 4.66 eV. Vibrational fine structures are denoted in the figure.

For some cluster sizes, similarities between the UPS spectra of $Ag_nO_2^-$ with those of the respective $Au_nO_2^-$ clusters can be found (Fig. 8). For $Ag_2O_2^-$ and $Au_2O_2^-$, broad features can be observed at lower binding energies followed by several narrower peaks. In the case of $Au_{12}O_2^-$ and

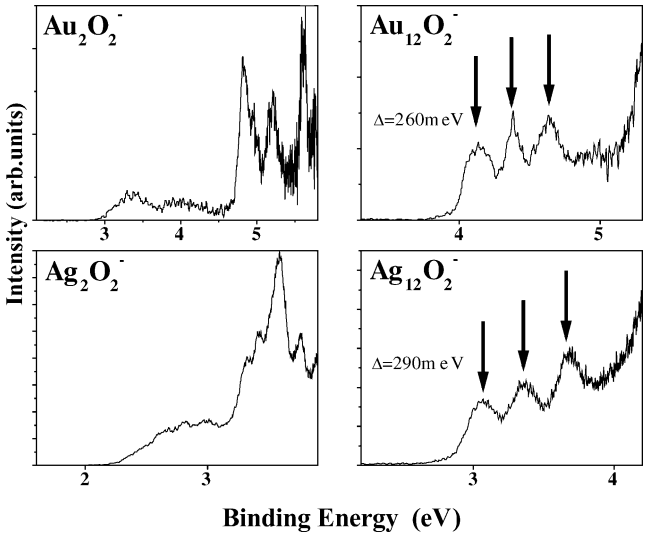

Fig. 8. UPS spectra of $Ag_2O_2^-$ and $Ag_{12}O_2^-$ are compared with those of the respective Au cluster anions. Similarities of $Ag_nO_2^-$ and the Au counterparts imply that O_2 chemisorption geometires on Ag and Au cluster anions should be analogous.

$Au_{12}O_2^-$, three distinct peaks are located at the lower binding energy regime. The valence band structures of these clusters are most likely dominated by the antibonding orbitals of oxygen (O_2-2π*), suggesting that the adsorption structures of O_2 on these Au and Ag cluster anions are analogous. These results again suggest that oxygen should be molecularly bound on these Ag cluster anions, like on the Au cluster anions.

The Au cluster anions smaller than Au_{21}^- have drawn particular attention due to their extraordinarily high catalytic activities for reactions involving oxygen adsorption, and it was found that the superoxo-species on the Au cluster anions are important reaction intermediates on Au-based catalysts. Since the oxygen chemisorption properties of the Ag cluster anions studied here are quite analogous to those of the catalytically active Au clusters, it is likely that Ag-nanoclusters can be as active as Au-clusters for those reactions in which molecular oxygen is an important intermediate, e.g., CO-oxidation and partial oxidation of hydrocarbons. In fact, Ag nanoparticles deposited on titania supports were found to be as reactive as Au nanoparticles on titania for CO-oxidation, and partial oxidation of hydrocarbons, which is in line with the results from the present work [33].

4.3. O_2 chemisorption on Cu cluster anions

Previously, Lee and Ervin studied O_2 chemisorption reactivities of Au, Ag and Cu cluster anions [43]. In the case of Cu, the even/odd-alternation was much less pronounced compared to the cases of Au and Ag cluster anions, i.e., not only even-numbered but also odd-numbered cluster anions are active towards O_2 chemisorption. Au and Ag clusters can react with only one O_2 molecule, whereas Cu clusters can possibly react with more than two O_2 molecules. It is well known that Cu bulk crystals easily react with oxygen forming Cu oxide. Cu monomer and Cu dimer anions can also efficiently dissociate O_2, suggesting that O_2 should dissociatively chemisorb on Cu cluster anions, regardless of the cluster size [86–88]. However, there were some indications that Cu cluster anions consisting of 5–10 atoms can interact less strongly than smaller Cu cluster anions. Cu cluster anions consisting of less than 5 atoms can react with more than 2 O_2 molecules, however, Cu_6^-–Cu_{10}^- can only react with one O_2 molecule [43]. Therefore, one cannot exclude the possibility to observe completely different chemical properties of these medium-sized Cu cluster anions from those of other Cu clusters, e.g., O_2 may molecularly chemisorb on Cu_n^- with n = 6–10.

Fig. 9 shows the UPS spectra of $Cu_6O_2^-$ and $Cu_7O_2^-$, which were produced by admission of O_2 into the PACIS source after Cu clusters formed and were cooled down to room temperature [56]. A mass spectrum of the reacted Cu clusters is also shown in Fig. 9c, indicating that there is almost no even/odd-alternation of the O_2 chemisorption reactivity. One can also see that the mass-resolution of the present work is high enough to resolve different isotopes of

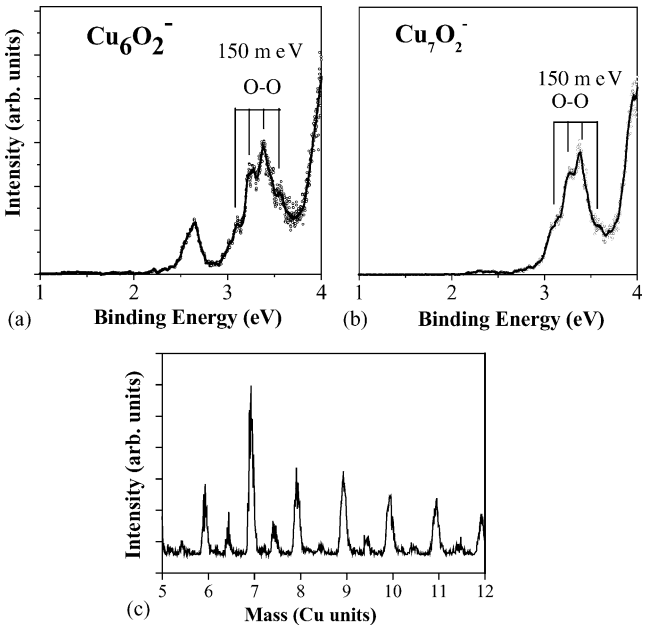

Fig. 9. UPS spectra of (a) $Cu_6O_2^-$ and (b) $Cu_7O_2^-$. The photon energy is 4.66 eV, and the vibrational fine structures are denoted in the figure. (c) Mass spectrum of the reacted Cu cluster anions.

Cu (Fig. 9c). For $Cu_6O_2^-$, no vibrational fine structure is resolved in the first peak at about 2.6 eV; however, features between 3 and 3.6 eV contain several equally spaced subpeaks, which should correspond to the vibrational frequency of a Cu_6O_2 neutral cluster. The peaks at 2.6 eV and 3–3.6 eV are attributed to the transitions from the ground state of the anion to the ground and the first excited state of the neutral, respectively. In principle, vibrational fine structures are expected to be present in both features; however, most likely, the too low intensity of the peak at 2.6 eV does not allow observation of the vibrational progressions in this feature, i.e., we can observe the vibrational frequency of the neutral Cu_6O_2 not in the ground state but in the first excited state. The periodicity of the fine structure between 3 and 3.6 eV in Fig. 9 a amounts to about 150 meV, corresponding to the O–O stretching frequency of a superoxo-species (O_2^-) [62,63]. This indicates the existence of an O–O bond in Cu_6O_2, i.e., O_2 does not dissociate on Cu_6^-. For $Cu_7O_2^-$, also, a 150 meV-periodicity can be observed in the UPS spectrum (Fig. 9b), indicative of the molecular chemisorption of O_2. In this case, the vibrational fine structure is present in the first peak from the lowest binding energy, indicating that this fine structure corresponds to the vibration of the neutral Cu_7O_2 in its ground state. It is important to mention that the features at the lowest binding energy range for metal clusters bound to O_2 contain significantly high contributions from the antibonding $2\pi^*$ orbitals of O_2, and therefore photoelectron detachments from these states should change the O–O bond length, yielding the vibrational progression of the O–O bond. It should be pointed out that our UPS spectra of CuO_2^- and $Cu_2O_2^-$ are consistent with previous ones from Wang et al., demonstrating the high reliability of our UPS spectra [86,87].

Our result indicates that at certain cluster sizes, Cu can become resistant towards oxide formation, since the dissociative chemisorption is the precursor state of the oxide formation [89]. As mentioned above, reactions of coinage metal cluster anions with oxygen can be explained within an electronic model, in which lower electron affinities of the neutral clusters facilitate metal to oxygen charge transfers of the anionic counterparts, yielding larger reactivities towards oxygen chemisorption. That Cu_6^- and Cu_7^- do not allow dissociation of the O–O bond, can be rationalized by the relatively high electron affinities of Cu_6 and Cu_7, hampering a metal to oxygen charge transfer, and ending up with the molecular chemisorption. In particular, Cu_7^- has a closed electronic shell configuration, having a high electron affinity of the neutral counterparts and a large gap between the HOMO and LUMO, which might explain the chemical inertness of this cluster [60]. However, these results are still surprising, considering that the electron affinities of Cu_6 and Cu_7 are much lower than those of other larger Cu clusters, which should dissociate O_2, and form Cu-oxide [60]. As aforementioned, reactivities of Cu_6^- and Cu_7^- towards O_2 chemisorption are much lower than those of Cu_n^- with n = 1–4, since these smaller clusters can react with more than two O_2 molecules, whereas Cu_6^- and Cu_7^- allow attachment of only one O_2 molecule on a cluster [43]. Our result that Cu_6^- and Cu_7^- do not allow dissociation of the O–O bonding, i.e., Cu_6^- and Cu_7^- interact less strongly than smaller Cu cluster anions, can reconcile the reactivity data of Lee and Ervin [43]. We are currently carrying out experiments on O_2 chemisorption reactivities of other Cu clusters, which are not studied so far using UPS.

The chemisorption properties of O_2 on Cu_6^- and Cu_7^- seem to be analogous to those of the Au cluster anions consisting of between 2 and 20 atoms, since the molecular chemisorption of oxygen was also observed for the even-numbered Au cluster anions. For the even-numbered Au cluster anions reacted with O_2, UPS spectra showed vibrational fine structures of O–O stretching frequencies, and the activated di-oxygen species were suggested to be important reaction intermediates. Based on our results in Fig. 9, it is suggestive that Cu clusters with certain sizes may be promising candidates for catalyzing those reactions, for which formation of activated di-oxygen species is important (such as low temperature CO-oxidation, and propylene epoxidation).

4.4. Hydrogen chemisorption on Au cluster anions

Besides O_2 chemisorption on metal clusters, hydrogen-metal cluster interaction is another important issue in heterogeneous catalysis. For example, Au nanoparticles are active towards various reactions, in which hydrogen plays an important role (e.g., propylene epoxidation) [31]. Note that the partial oxidation of hydrocarbons generally occurs in O_2 and H_2 atmospheres, which most likely form hydrogen peroxide species on the surface [31]. Studies on the interactions be-

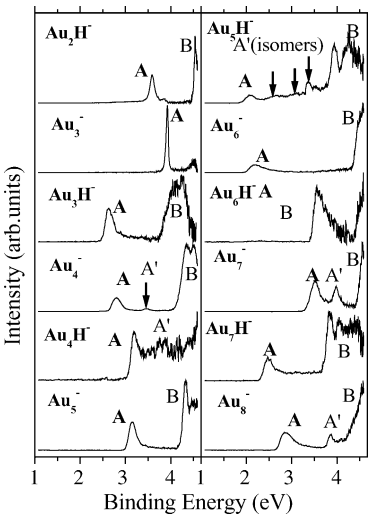

Fig. 10. UPS spectra of $Au_{n-1}H^-$ are compared with those of Au_n^- (n = 3–8). The photon energy is 4.66 eV.

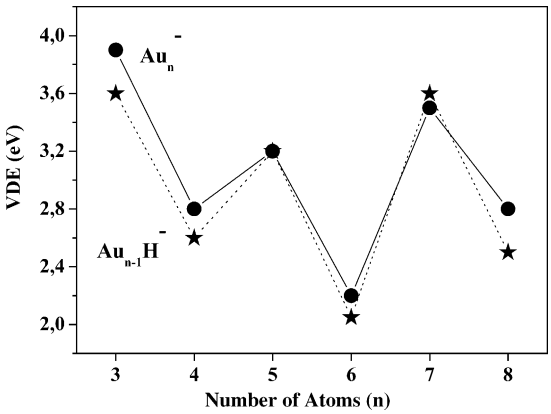

Fig. 11. The vertical detachment energies (VDE) of $Au_{n-1}H^-$ and Au_n^- as a function of cluster size.

tween hydrogen and Au clusters are essential to unveil the origin of the unusual chemical activities of Au.

Fig. 10 displays spectra of Au_n^- and $Au_{n-1}H^-$ clusters for n = 3–8, showing that the spectra of the $Au_{n-1}H^-$ clusters are similar to those of the respective Au_n^- clusters [57]. Linear Au_3^- has a relatively high vertical detachment energy (feature A at 3.9 eV), which is also observed for Au_2H- (feature A at 3.6 eV). Following the even/odd alternation, the VDE is relatively low for Au_4^- (2.8 eV) as it is for Au_3H^- (2.6 eV). The spectra of the 4-atom clusters are very similar except for the small differences in binding energies of the d-orbital emission (features marked B). For the 5-atom clusters, the VDEs of both clusters are again similar (peaks marked A), but the spectrum of Au_4H^- shows some weak superimposed maxima in the higher binding energy regime (marked A′), which cannot be found for Au_5^-. A similar behaviour is observed for the 6-atom clusters. The main features A and B are at comparable BEs for Au_6^- and Au_5H^-, but in the spectrum of Au_5H^- there are several additional weak peaks (marked A′, arrows). We assign these weak features to different, less abundant isomers. In the spectrum of Au_4^- a weak feature (A′) is visible, which is assigned to an almost degenerate isomer of the tetramer anion. The topic of different coexisting isomers of Au_nH^- clusters and their formation has been addressed in a recent paper [90–92].

For the larger clusters displayed in Fig. 10, the even/odd-alternation continues and the shell closing expected at 8 electrons (Au_7^-, Au_6H^-) manifests itself in a relatively high VDE. For these larger clusters (n = 7, 8) the similarity between the spectra of the $Au_{n-1}H^-$ and Au_n^- clusters is again obvious, if we tentatively assign weak additional peaks (marked A′) to different isomers. In Fig. 11, the VDEs are plotted for the $Au_{n-1}H^-$ and Au_n^- clusters supporting the similarity of the electronic structures of these clusters. The electronic structures of these clusters are determined by the number of delocalized electrons and this number is not changed, if a Au atom is replaced by a monovalent atom, H.

Electronic structures of simple s/p metal clusters (coinage and alkali metals) are often described by the electron shell model, in which the s electrons from each atom form delocalized electronic shells in a cluster [93]. According to the electron shell model, closed shell configurations form when the number of valence electrons is 2, 8, 18, . . ., which has been also experimentally confirmed. The electron shell model is valid not only for homonuclear clusters, but also for alloy clusters, such as Au_nCs_m clusters [94–100]. Our result in Fig. 11 suggests that here, H acts like an alkali or a coinage metal atom.

For number of Au atoms higher than 3, electronic structures of Au_n^- and $Au_{n-1}H^-$ were shown to be similar (Fig. 10). One may assume that the geometries of $Au_{n-1}H^-$ and Au_n^- are also similar, since there is a strong coupling between geometric and electronic structures. This assumption can be confirmed by comparison with previous results from theoretical calculations, in which energetics and geometric structures of Au_nH^- were studied. The case with the most pronounced similarity of the photoelectron spectra is n = 4: the spectra of Au_4^- and Au_3H^-. For Au_4^- theory predicts a planar structure with a base triangle of three Au atoms and a fourth atom attached at the corner of the triangle [91]. The same structure has been calculated for Au_3H^- with the H replacing the top Au atom with a slightly shorter bond length [90]. For the cases of Au_6^- and Au_5H^- the calculated geometries are very similar, too: Au_6^- has a planar triangular structure, and Au_5H^- has a similar structure with the H atom replacing a corner Au atom [90,91]. For those two sizes (n = 4, 6) the geometries of the bare and hydrogenated cluster anions are similar as are the photoelectron spectra.

In our photoelectron spectra we observe the uppermost occupied orbitals of the cluster valence band. This binding energy regime is dominated by the (s, p)-derived density of states and these states can be viewed as a superposition of 6s and 6p orbitals of the Au atoms in the cluster. If one atom is removed, the hole manifold of states is changed as proven

by the pronounced size dependence of the spectra of the bare Au_n^- clusters. The manifold of s/p-derived orbitals remains almost unchanged upon replacement of an Au atom by another atom, only when the new atom contributes to the manifold of states in a manner like a Au atom does, resulting in no changes in electronic and geometric structures. Since we only observe the uppermost occupied orbitals, changes might be occurring for s/p-derived orbitals at higher binding energies, especially for the lowest molecular orbital of the conduction "band". However, it seems that the HOMOs are very similar in shape and symmetry for $Au_{n-1}H^-$ and Au_n^-.

Previously, CO was shown to be a two-electron donor on coinage metal clusters [101–104]. One of the important consequences of this result is that coadsorption of CO with other electron-accepting adsorbates like oxygen can be non-competitive but cooperative [37]. Our result shows that on Au clusters, hydrogenation provides an electron to the valence electron pool of Au clusters, which can result in cooperative adsorption between H and oxygen, analogous to the case of CO and O_2 coadsorption on Au cluster anions. This can be closely related to the high activities of Au clusters towards various reactions in which H adsorption is involved. For the partial oxidation of propylene in H_2 and O_2 environments, hydrogen peroxide (H_2O_2) is believed to be an important reaction intermediate. To maximize the yield of hydrogen peroxide, the rates of the $H+O_2 \rightarrow HOO$ and $H + O_2H \rightarrow HOOH$ reactions should be enhanced. For Pt-group metals, hydrogen adsorption lowers the rate of oxygen adsorption, or vice versa, most likely because H is an electron-acceptor like oxygen, leading to the competitive adsorption of both reagents [105]. Consequently, the HOOH formation involves a high activation barrier. On Au clusters, it can be facilitated as a consequence of the cooperative adsorption of H and O_2. It is worth mentioning that Au clusters do not react with H_2 but only with H, implying that in real catalysis, dissociation of H_2 occurs on defects of oxide support materials, and the atomic H can then diffuse onto the Au particles, or H_2 dissociate at the oxide/Au boundaries. Alternatively, H_2 only dissociates in the presence of the precovered oxygen on Au nanoclusters. It is important to note that in heterogeneous catalysis, the cooperative chemisorption of hydrogen and oxygen was found, which may be in line with the results in Figs. 10 and 11 [106].

5. Summary and outlook

In the present article, recent results on chemisorption properties of coinage metal clusters using mass spectroscopy in combination with UPS are demonstrated. It was shown that oxygen often forms di-oxygen species on coinage metal cluster anions, and di-oxygen species are suggested to be important reaction intermediates for various reactions catalyzed by coinage metal clusters such as low temperature CO-oxidation and partial oxidation of hydrocarbons. For H chemisorption on Au cluster anions, H was found to act as a one-electron donor, which may play an important role for forming hydrogen peroxide species on Au cluster anions.

The question may be raised, whether the results from the gas phase clusters can be also relevant for real catalysis, consisting of metal nanoparticles supported by oxide surfaces. It should be mentioned that very recent studies using Au particles on titania surfaces identified molecularly bound oxygen species, in line with our results shown here [107]. For coadsorption of hydrogen and oxygen on Au-based catalysts, hydroperoxide species (HOOH) could be identified, also suggesting that oxygen chemisorbs nondissociatively on Au nanoparticles supported by oxide surfaces, consistent with the gas phase cluster data [108]. This suggests that gas phase clusters can serve as important model systems to obtain a better understanding of elementary steps of heterogeneous catalysis. Gas phase clusters can be easily mass selected, and therefore size dependent changes of chemical properties can be followed on atomic scale. Moreover, gas phase data can be more easily compared with theoretical results.

Ultraviolet Photoelectron Spectroscopy can be a powerful tool to further identify important reaction intermediates on gas phase clusters, e.g., coadsorption of CO and O_2 may form CO_3 and H_2 and O_2 can form HOOH on metal clusters, which can be identified using photoelectron spectroscopy.

To follow reaction paths on a real time scale, Time-Resolved two Photon Photoelectron Emission (TR-2PPE) spectroscopy experiments can be carried out, which has been done on pure metal clusters have been carried out [109,110]. Investigations on chemisorption, desorption, and catalytic reactions on metal clusters employing TR-2PPE studies are under way. To shed light on the metal support interactions, comparative studies on free and deposited clusters should be further performed.

Acknowledgement

I gratefully acknowledge the financial support from Deutsche Forschungsgemeinschaft (DFG). I would like to express my special gratitude to Gerd Ganteför, Puru Jena and their co-workers for support and cooperation. Nils Bertram is acknowledged for proofreading of the manuscript.

References

[1] H. Kietzmann, J. Morenzin, P.S. Bechthold, G. Ganteför, W. Eberhardt, J. Chem. Phys. 109 (1998) 2275.
[2] J.L. Elkind, F.D. Weiss, J.M. Alford, R.T. Laaksonen, R.E. Smalley, J. Chem. Phys. 88 (1998) 5215.
[3] M.D. Morse, M.E. Geusic, J.R. Heath, R.E. Smalley, J. Chem. Phys. 83 (1985) 2293.
[4] M.R. Zakin, R.O. Brickman, D.M. Cox, A. Kaldor, J. Chem. Phys. 88 (1988) 3555.
[5] R.L. Whetten, M.R. Zakin, D.M. Cox, D.J. Trevor, A. Kaldor, J. Chem. Phys. 85 (1986) 1697.
[6] D.M. Cox, K.C. Reichmann, D.J. Trevor, A. Kaldor, J. Chem. Phys. 88 (1988) 111.

[7] S.A. Mitchell, D.M. Rayner, T. Bartlett, P.A. Hackett, J. Chem. Phys. 104 (1996) 4012.
[8] L. Holmgren, M. Andersson, A. Rosĕn, J. Chem. Phys. 109 (1998) 3232.
[9] M. Engeser, T. Weiske, D. Schröder, H. Schwarz, J. Phys. Chem. A 107 (2003) 2855.
[10] K. Koszinowski, D. Schröder, H. Schwarz, Organometallics 22 (2003) 3809.
[11] K. Koszinowski, D. Schröder, H. Schwarz, J. Phys. Chem. A 107 (2003) 4999.
[12] S.R. Tennison, in: J.R. Jenningns (Ed.), Catalytic Ammonia Synthesis, first ed., Plenum, New York, 1991.
[13] D.A. King, Woodruff (Eds.), The Chemical Physics of Solid Surfaces and Heterogeneous Catalysis, vol. 3A, Elservier, Amsterdam, 1990.
[14] G.A. Somorjai, Introduction to Surface Chemistry and Catalysis, Wiley, New York, 1994.
[15] K. Christmann, Introduction to Surface Physical Chemistry, Steinkopff, Darmstadt, Springer Verlag, New York, 1991.
[16] H.P. Bonzel, H.J. Krebs, Surf. Sci. 117 (1982) 639.
[17] D.W. Blakely, E. Kozak, N.A. Sexton, G.A. Somorjai, J. Vac. Sci. Technol. 13 (1976) 1091.
[18] D.W. Goodman, J. Phys. Chem. 100 (1996) 13090.
[19] T.P.St. Clair, D.W. Goodman, Top. Catal. 123 (2000) 5.
[20] M. Bäumer, H.J. Freund, Prog. Surf. Sci. 61 (1999) 127.
[21] M. Valden, X. Lai, D.W. Goodman, Science 281 (1998) 1647.
[22] M. Haruta, S. Tsubota, T. Kobayashi, H. Kageyama, M.J. Genet, B. Delmon, J. Catal. 144 (1993) 175.
[23] T.V. Choudhary, D.W. Goodman, Top. Catal. 21 (2002) 25.
[24] F. Boccuzzi, A. Chiorino, J. Phys. Chem. B 104 (2000) 5414.
[25] Y. Iizuka, H. Fujiki, N. Yamauchi, T. Chijiiwa, S. Arai, S. Tsubota, M. Haruta, Catal. Today 36 (1997) 115.
[26] Y. Iizuka, T. Tode, T. Takao, K. Yatsu, T. Takeuchi, S. Tsubota, M. Haruta, J. Catal. 187 (1999) 50.
[27] M. Okumura, J.M. Coronado, J. Soria, M. Haruta, J.C. Conesa, J. Catal. 203 (2001) 168.
[28] H. Liu, A.I. Kozlov, A.P. Kozlova, T. Shido, K. Asakura, Y. Iwasawa, J. Catal. 185 (1999) 252.
[29] J.-D. Grunwaldt, M. Maciejewski, O.S. Becker, P. Fabrizioli, A. Baiker, J. Catal. 186 (1999) 458.
[30] F. Boccuzzi, A. Chiorino, M. Manzoli, Surf. Sci. 454–456 (2000) 942.
[31] T. Hayashi, K. Tanaka, M. Haruta, J. Catal. 178 (1998) 566.
[32] A. Cho, Science 299 (2003) 1684.
[33] L.A. de Oliveira, A. Wolf, F. Schüth, Catal. Lett. 73 (2001) 157.
[34] A. Sanchez, S. Abbet, U. Heiz, W.-D. Schneider, H. Häkkinen, R.N. Barnett, U. Landman, J. Phys. Chem. A 103 (1999) 9573.
[35] U. Heiz, W.-D. Schneider, J. Phys. D: Appl. Phys. 33 (2000) R85.
[36] H. Häkkinen, S. Abbet, A. Sanchez, U. Heiz, U. Landman, Angew. Chem. Int. Ed. 42 (2003) 1297.
[37] W.T. Wallace, R.L. Whetten, J. Am. Chem. Soc. 124 (2002) 7499.
[38] B.E. Salisbury, W.T. Wallace, R.L. Whetten, Chem. Phys. 262 (2000) 131.
[39] M.L. Kimble, A.W. Castleman Jr., R. Mitrić, C. Bürgel, V. Bonačić-Koutecký, J. Am. Chem. Soc. 126 (2004) 2526.
[40] J. Hagen, L.D. Socaciu, J. Le Roux, D. Popolan, T.M. Bernhardt, L. Wöste, R. Mitrić, H. Noack, V. Bonačić-Koutecký, J. Am. Chem. Soc. 126 (2004) 3442.
[41] J. Hagen, L.D. Socaciu, M. Elijazyfer, U. Heiz, T.M. Bernhardt, L. Wöste, Phys. Chem. Chem. Phys. 4 (2002) 1707.
[42] L.D. Socaciu, J. Hagen, T.M. Bernhardt, L. Wöste, U. Heiz, H. Hakkinen, U. Landman, J. Am. Chem. Soc. 125 (2003) 10437.
[43] T.H. Lee, K.M. Ervin, J. Phys. Chem. 98 (1994) 10023.
[44] T.S. Kim, J.D. Stiehl, C.T. Reeves, R.J. Meyer, C.B. Mullins, J. Am. Chem. Soc. 125 (2003) 2018.
[45] N. Lopez, J.K. Norskov, J. Am. Chem. Soc. 124 (2002) 11262.
[46] H. Häkkinen, U. Landman, J. Am. Chem. Soc. 123 (2001) 9704.
[47] G. Mills, M.Y. Gordon, H. Metiu, Chem. Phys. Lett. 359 (2002) 493.
[48] Z.-P. Liu, P. Hu, A. Alavi, J. Am. Chem. Soc. 124 (2002) 14770.
[49] W.T. Wallace, A.J. Leavitt, R.L. Whetten, Chem. Phys. Lett. 368 (2003) 774.
[50] S.A. Varganov, R.M. Olson, M.S. Gordon, G. Mills, H. Metiu, Chem. Phys. Lett. 368 (2002) 778.
[51] V.A. Bondzie, S.C. Park, C.T. Campbell, J. Vac. Sci. Technol. A 17 (1999) 1717.
[52] D. Stolcic, M. Fischer, G. Ganteför, Y.D. Kim, Q. Sun, P. Jena, J. Am. Chem. Soc. 125 (2003) 2848.
[53] Y.D. Kim, M. Fischer, G. Ganteför, Chem. Phys. Lett. 377 (2003) 170.
[54] Q. Sun, P. Jena, Y.D. Kim, M. Fischer, G. Ganteför, J. Chem. Phys. 120 (2004) 6510.
[55] Y.D. Kim, G. Ganteför, Chem. Phys. Lett. 383 (2004) 83.
[56] F.v. Gynz-Rekowski, N. Bertram, G. Ganteför, Y.D. Kim, J. Phys. Chem. A (2004), submitted for publication.
[57] S. Buckart, Y.D. Kim, G. Ganteför, P. Jena, J. Am. Chem. Soc. 125 (2003) 14205.
[58] C.Y. Cha, G. Ganteför, W. Eberhardt, Rev. Sci. Instrum. 63 (1992) 5661.
[59] S. Burkart, N. Blessing, B. Klipp, J. Müller, G. Ganteför, G. Seifert, Chem. Phys. Lett. 301 (1999) 546.
[60] K.J. Taylor, C.L. Pettiette-Hall, O. Cheshnovsky, R.E. Smalley, J. Chem. Phys. 96 (1992) 3319.
[61] K. Koswinowski, D. Schröder, H. Schwarz, Organometallics 23 (2004) 1132.
[62] H. Steiniger, S. Lehwald, H. Ibach, Surf. Sci. 123 (1982) 1.
[63] N.D. Shinn, T.E. Madey, Surf. Sci. 176 (1986) 635.
[64] B. Yoon, H. Häkkinen, U. Landman, J. Phys. Chem. 107 (2003) 4066.
[65] J. Li, X. Li, H.-J. Zhai, L.-S. Wang, Science 299 (2003) 864.
[66] B.K. Rao, P. Jena, S. Burkart, G. Ganteför, G. Seifert, Phys. Rev. Lett. 86 (2001) 692.
[67] T. Engel, G. Ertl, Adv. Catal. 28 (1979) 1.
[68] Y.D. Kim, D. Stolcic, M. Fischer, G. Ganteför, J. Chem. Phys. 119 (2003) 10307.
[69] Y.D. Kim, D. Stolcic, M. Fischer, G. Ganteför, Chem. Phys. Lett. 380 (2003) 359.
[70] Y.D. Kim, G. Ganteför, Chem. Phys. Lett. 382 (2003) 644.
[71] D.V. Yandulov, R.R. Schrock, Science 301 (2003) 76.
[72] D.D. Eley, Adv. Catal. Rel. Subj. 1 (1948) 157.
[73] C.H.F. Peden, D.W. Goodman, M.D. Weisel, F.M. Hoffmann, Surf. Sci. 253 (1991) 44.
[74] F.M. Hoffmann, M.D. Weisel, C.H.F. Peden, Surf. Sci. 253 (1991) 59.
[75] C. Stampfl, M. Scheffler, Phys. Rev. Lett. 78 (1997) 1500.
[76] K. Koszinowski, D. Schröder, H. Schwarz, Chem. Phys. Chem. 4 (2003) 1233.
[77] Z. Yang, R. Wu, D.W. Goodman, Phys. Rev. B 61 (2000) 14066.
[78] F. Furche, R. Ahlrichs, P. Weiss, C. Jakob, S. Gilb, T. Bierweiler, M.M. Kappes, J. Chem. Phys. 117 (2002) 6982.
[79] S. Rabii, C.Y. Yang, Chem. Phys. Lett. 105 (1984) 480.
[80] A.F. Ramos, R. Arratia-Perez, G.L. Malli, Phys. Rev. B 35 (1987) 3790.
[81] K. Balasubramanian, K.K. Das, Chem. Phys. Lett. 186 (1991) 577.
[82] C.W. Bauschlicher Jr., Chem. Phys. Lett. 156 (1989) 91.
[83] H. Schwarz, Angew. Chem. Int. Ed. 42 (2003) 4442.
[84] N. Bartlett, Gold. Bull. 31 (1998) 22.
[85] K. Koszinowski, D. Schröder, H. Schwarz, Angew. Chem. Int. Ed. 43 (2004) 121.
[86] L.S. Wang, H. Wu, S.R. Desai, L. Lou, Phys. Rev. B 53 (1996) 8028.
[87] H. Wu, S.R. Desai, L.S. Wang, J. Phys. Chem. 101 (1997) 2103.
[88] C.T. Campbell, K.A. Daube, J.M. White, Surf. Sci. 182 (1987) 458.
[89] A.P. Seitsonen, H. Over, Science 297 (2002) 2003.

[90] D. Fischer, W. Andreoni, A. Curioni, H. Grönbeck, S. Burkart, G. Ganteför, Chem. Phys. Lett. 361 (2002) 389.
[91] H. Häkkinen, U. Landman, Phys. Rev. B 62 (2000) R2287.
[92] H. Häkkinen, M. Moseler, U. Landman, Phys. Rev. Lett. 89 (2002) 033401.
[93] W.A. Heer, Rev. Mod. Phys. 65 (1993) 611.
[94] E. Janssens, H. Tanaka, S. Neukermans, R.E. Silverans, P. Lievens, New J. Phys. 5 (2003) 46.1.
[95] T.P. Martin, T. Bergmann, H. Göhlich, T. Lange, Chem. Phys. Lett. 172 (1990) 209.
[96] X. Li, H. Wu, X.B. Wang, L.-S. Wang, Phys. Rev. Lett. 81 (1998) 1909.
[97] U. Heiz, A. Vayloyan, E. Schuhmacher, C. Yeretzian, M. Stener, P. Gisdakis, N. Rösch, J. Chem. Phys. 105 (1996) 5574.
[98] O.C. Thomas, W.-J. Zheng, T.P. Lippa, S.-J. Xu, S.A. Lyapustina, K.H. Bowen Jr., J. Chem. Phys. 114 (2001) 9895.
[99] K. Hoshino, K. Watanabe, Y. Konishi, T. Taguwa, A. Nakajima, K. Kaya, Chem. Phys. Lett. 231 (1994) 499.
[100] C.J. Yeretzian, Phys. Chem. 99 (1995) 123.
[101] R.H. Crabtree, The Organometallic Chemistry of the Transition Metals, Wiley, New York, 1988.
[102] M.A. Nygren, P.E.M. Siegbahn, C. Jin, T. Guo, R.E. Smalley, J. Chem. Phys. 95 (1991) 6181.
[103] L. Panas, J. Schüle, P. Siegbahn, U. Wahlgren, Chem. Phys. Lett. 149 (1988) 265.
[104] M.A. Nygren, E.M. Siegbahn, J. Phys. Chem. 96 (1992) 7579.
[105] T. Mitsui, M.K. Rose, E. Fomin, D.F. Ogletree, M. Salmeron, Surf. Sci. 511 (2002) 259.
[106] S. Naito, M. Tanimoto, J. Chem. Soc. Chem. Commun. (1988) 832.
[107] J.D. Stiehl, T.S. Kim, S.M. McClure, C.B. Mullins, J. Am. Chem. Soc. 126 (2004) 1606.
[108] C. Sivadinarayana, T.V. Choudhary, L.L. Daemen, J. Eckert, D.W. Goodman, J. Am. Chem. Soc. 126 (2004) 38.
[109] M. Niemietz, P. Gerhardt, G. Ganteför, Y.D. Kim, Chem. Phys. Lett. 380 (2003) 99.
[110] P. Gerhardt, M. Niemietz, Y.D. Kim, G. Ganteför, Chem. Phys. Lett. 382 (2003) 454.